IEEE Photonics Journal
An IEEE Photonics Society Publication

Continuously Tunable Microwave Photonic Notch Filter With a Complex Coefficient

Volume 3, Number 3, June 2011

Wei Li
Ning Hua Zhu, Member, IEEE
Li Xian Wang

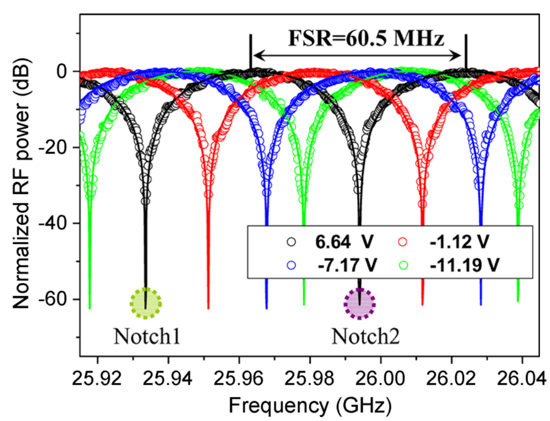

DOI: 10.1109/JPHOT.2011.2149509
1943-0655/$26.00 ©2011 IEEE

IEEE photonics SOCIETY
IEEE

Continuously Tunable Microwave Photonic Notch Filter With a Complex Coefficient

Wei Li, Ning Hua Zhu, *Member, IEEE*, and Li Xian Wang

State Key Laboratory on Integrated Optoelectronics, Institute of Semiconductors, Chinese Academy of Sciences, Beijing 100083, China

DOI: 10.1109/JPHOT.2011.2149509

Manuscript received April 5, 2011; revised April 21, 2011; accepted April 25, 2011. Date of publication May 5, 2011; date of current version May 17, 2011. Corresponding author: W. Li (e-mail: liwei05@semi.ac.cn).

Abstract: This paper presents a continuously tunable microwave photonic notch filter with a complex coefficient. The complex coefficient is generated using a radio-frequency (RF) phase shifter that consists of a dual-parallel Mach–Zehnder modulator (DPMZM) and a tunable optical bandpass filter (TBPF). By simply controlling the bias voltage of the DPMZM, the frequency response of the filter can be continuously tuned over a full free spectral range (FSR) without changing the shape of the frequency response.

Index Terms: Microwave photonic filter, microwave photonics signal processing, radio-frequency (RF) phase shifter.

1. Introduction

Microwave photonic filters (MPFs) have attracted considerable attention during the past few years due to their immunity to electromagnetic interference, their wide range of potential applications, and their advantages in terms of bandwidth, tunability, and reconfigurability, as compared with traditional radio-frequency (RF) circuits [1]. In general, MPFs are based on the multitap delay line concept. In order to avoid optical interferences and have a configuration free from the environmental variation, various methods have been proposed to operate the MPF in the incoherent regime, such as keeping the laser coherence time smaller than the optical delay time [2], using multiple optical sources [3]–[5], or making the state of polarization of the optical signals be orthogonal [6]. Recently, an optical comb source and a dispersive medium were used to implement tunable programmable MPFs [7]. Compared with MPFs based on a multiple optical source, MPFs using a single optical source are attractive due to cost issues. In [8], a switchable MPF was realized using a single optical source and a pair of intensity modulators. A recent upgrade of this proposal is based on single-wavelength optical source and phase-intensity hybrid modulation [9]. However, for MPFs working in the incoherent regime, only positive coefficients can be realized since the intensity is always positive, which results in a low-pass filter. To realize bandpass or high-pass MPFs, negative coefficients are need. In [10] and [11], MPFs with switchable positive or negative tap coefficients were demonstrated using fiber Bragg gratings (FBGs) [10] and tunable optical bandpass filters (TBPFs) [11]. Moreover, much effort has been made to implement tunable filter structures. The tunability is usually realized by adjusting the time delay difference, which results in simultaneous undesirable changes of the free spectral range (FSR) and the shape of the frequency response [12]–[14]. This problem can be solved by using microwave photonic phase shifters [15] that are capable of providing a tunable phase shift up to full 360° that remains constant over the RF region of interest or, in other word, using MPFs with complex coefficients. So far, two-tap microwave

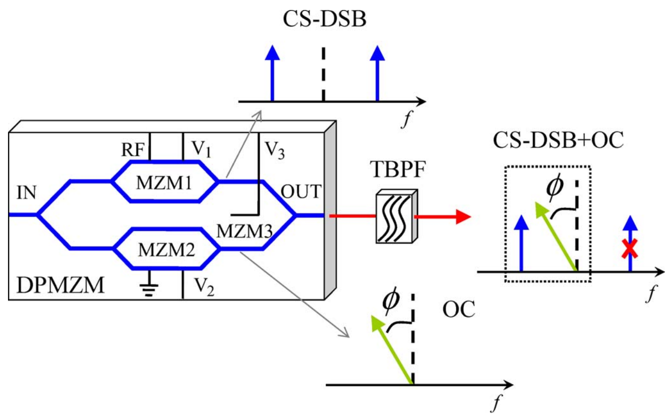

Fig. 1. RF phase shifter, along with the schematic optical spectra at different locations.

notch filters with one tap using an RF phase shifter have been implemented by several techniques, such as stimulated Brillouin scattering (SBS) [16], coherent population oscillations [17], silicon-on-insulator microring resonators [18], and all-optical differentiator [19]. In [16], however, to stimulate the SBS, a 20-km single-mode fiber was used, which makes the system bulky. The configuration of the RF phase shifter demonstrated in [15] is complex due to the use of too many components. In [19], the RF phase shifter can only realize a 180° phase shift, which results in a half FSR tuning range of the MPF.

In this paper, we demonstrate a novel and simple microwave photonic notch filter with a complex coefficient. The phase of the RF signal can be continuously shifted over a full 360° range using a dual-parallel Mach–Zehnder modulator (DPMZM) and a TBPF. Therefore, the filter can be tuned over an entire FSR, while the shape of the frequency response remains unaltered.

2. Principles of Operation

The key component in our microwave photonic notch filter is a frequency independent RF phase shifter, which was implemented by a commercial *x*-cut integrated DPMZM (Photline MXIQ-LN-40) and a TBPF as shown in Fig. 1. The DPMZM is structured as two MZMs (MZM1 and MZM2) set in parallel and forming a third MZM (MZM3). In the DPMZM, MZM1 was fed by an RF signal with peak amplitude of V_m and frequency of f_m and was biased at null point to implement carrier suppressed-double sideband (CS-DSB) modulation. The optical field from MZM1 is given by [20]

$$\begin{aligned} E_1 &= \frac{1}{2\sqrt{2}}E_{in}\exp\left(j2\pi f_0 t + j\beta\cos 2\pi f_m t - j\frac{\pi}{2}\right) + \frac{1}{2\sqrt{2}}E_{in}\exp\left(j2\pi f_0 t - j\beta\cos 2\pi f_m t + j\frac{\pi}{2}\right) \\ &= E_{in}\sin(\beta\cos 2\pi f_m t)\exp(j2\pi f_0 t)/\sqrt{2} \\ &= \frac{E_{in}}{2\sqrt{2}}J_1(\beta)\exp[j2\pi(f_0 - f_m)t] + \frac{E_{in}}{2\sqrt{2}}J_1(\beta)\exp[j2\pi(f_0 + f_m)t] \end{aligned} \quad (1)$$

where $E_{in}\exp(j2\pi f_0 t)$ is the input optical field, f_0 is the frequency of the optical carrier (OC), $J_1(\beta)$ is the first-order Bessel function of the first kind, $\beta = (\pi/2)V_m/V_{\pi 1}$, and $V_{\pi 1}$ is the half-wave voltage of MZM1. The RF port of the MZM2 was shorted and the bias voltage of the MZM2 was set at maximum transmission point to allow the OC to pass through. The optical field from MZM2 can be written by

$$E_2 = E_{in}\exp(j2\pi f_0 t)/\sqrt{2}. \quad (2)$$

Both the optical signals from MZM1 and MZM2 are combined in MZM3 to generate a CS-DSB+OC signal. A phase difference ϕ_3 between CS-DSB and OC signals was then achieved by controlling the dc bias of MZM3, V_3. The optical field from DPMZM can be expressed as

$$E_{out1} = [E_1 + E_2 \exp(j\phi_3)]/\sqrt{2} \tag{3}$$

where $\phi_3 = \pi(V_3 - V_{\text{offset}})/V_{\pi 3}$, $V_{\pi 3}$ is the half-wave voltage of MZM3, and V_{offset} is the offset voltage when $\phi_3 = 0$. In order to achieve single-sideband (SSB) modulation, a TBPF was used to remove the upper frequency sideband of the CS-DSB+OC signal. Therefore, the optical field from the output of the TBPF is given by

$$E_{out2} = \frac{E_{in}}{4} J_1(\beta) \exp[j2\pi(f_0 - f_m)t] + \frac{E_{in}}{2} \exp[j(2\pi f_0 t + \phi_3)]. \tag{4}$$

Then, if this optical signal were detected in a photodetector (PD), the RF signal would be proportional to

$$i(t) = E_{out2} \cdot E^*_{out2} \propto E^2_{in} \cdot J_1(\beta) \cdot \cos(2\pi f_m t + \phi_3). \tag{5}$$

It can be seen that the RF phase shift ϕ_3 is a linear function of the bias voltage V_3, which is independent of the RF.

The transfer function of a two-tap incoherent microwave photonic notch filter is given by

$$H(f) = a_1 + a_2 \cdot \exp(-j2\pi f T) \tag{6}$$

where a_1 and a_2 are the filter taps coefficients that can be real or complex, and T is the basic delay of the filter. When the complex coefficients are changed by introducing a phase shift ϕ_3 to one arm, the frequency response of the filter can be expressed as

$$H'(f) = a_1 + a_2 \exp(j\phi_3) \cdot \exp(-j2\pi f T) = H\left(f - \frac{\phi_3}{2\pi T}\right). \tag{7}$$

The notch position of the filter is changed by $\phi_3/2\pi T$. It must be pointed out that, by adjusting V_3, the notch position of the filter is varied while maintaining the shape and the FSR of the frequency response unchanged, since the basic time delay between the two arms of the filter is fixed.

3. Experiments and Results

We first investigate the phase shift property of the photonic RF phase shifter based on the DPMZM and the TBPF. In this experiment, the optical signal from a tunable laser source (TLS) emitting at 1549.935 nm with optical power of 12 dBm was fed to the DPMZM. The MZM1 and MZM2 were biased at $V_1 = -7.45$ V and $V_2 = -3.65$ V, respectively, to achieve a CS-DSB+OC signal. The TBPF with 3-dB bandwidth of 0.8 nm was attached to the output port of the DPMZM to remove the upper frequency sideband of the CS-DSB+OC signal. The optical spectra without and with the TBPF are shown in Fig. 2. The modulation frequency of the DPMZM was 26 GHz. As can be seen, the sideband suppression ratio is 43 dB. The transfer function of the TBPF is also shown in Fig. 2, which was measured with the help of the amplified spontaneous emission (ASE) optical signal from an erbium-doped fiber amplifier (EDFA). The roll-off of the TBPF was measured to be 196 dB/nm. The TBPF introduced 4 and 5.3 dB optical power attenuations to the lower frequency sideband and the OC, respectively, as shown in Fig. 2. Note that the OC was located at the high-frequency slope of the TBPF transfer function and, thus, suffered more attenuation than the lower sideband. Meanwhile, the TBPF also introduced a phase shift φ_{TBPF} to the OC [2]. When the SSB modulated optical signal, as shown in Fig. 2, was detected by a 45-GHz PD, the RF signal was recovered. We used a 40-GHz vector network analyzer (VNA) to measure the phase shift of the recovered RF signal. The VNA was calibrated when $V_3 = 1.1$ V. Fig. 3(a) shows a nearly linear phase shift of the 26-GHz RF signal with respect to the control voltage (V_3) of the DPMZM. A full 360° RF phase shift was achieved when the dc bias of the DPMZM was tuned from -12.03 to 15.28 V, which was determined by $V_{\pi 3}$ of the MZM3. The measured phase shift versus RF for different bias voltage V_3 is shown in Fig. 3(b). As expected from (5), the measured phase shift is independent of the RF.

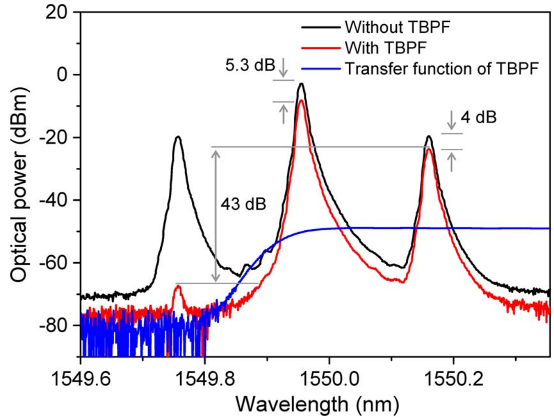

Fig. 2. Measured optical spectra without and with the TBPF, as well as the transfer function of the TBPF.

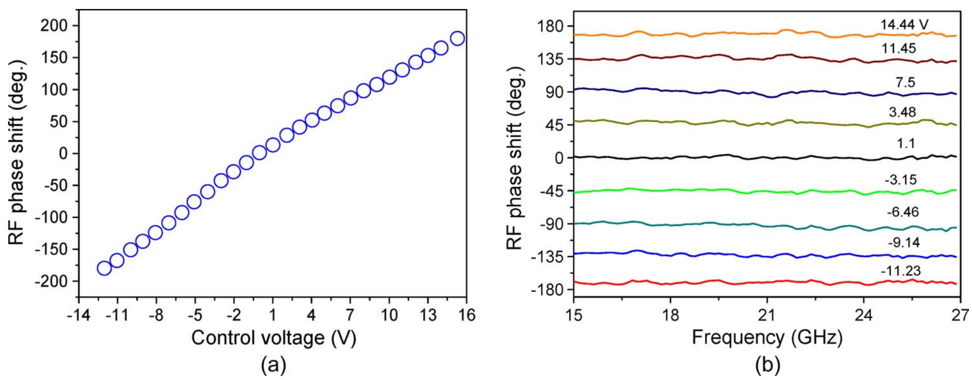

Fig. 3. (a) Measured phase shift of the 26-GHz RF signal with respect to the bias voltage V_3 of the DPMZM and (b) measured phase shift versus RF for different bias voltage V_3.

Therefore, it is possible to use this RF phase shifter to generate a complex coefficient in the two-tap incoherent microwave photonic notch filter.

As shown in Fig. 2, the OC was located at the high-frequency slope of the TBPF transfer function in order to block the upper frequency sideband. The TBPF imparted a fixed phase shift on OC. For lower RFs, however, the phase of the lower optical sideband will also be changed due to the TBPF-induced phase shift. Moreover, this phase shift is frequency dependent. Therefore, the bandwidth of the RF phase shifter is limited by the roll-off property of the TBPF and the bandwidth of the DPMZM employed. The frequency response of the RF phase shifter, as shown in Fig. 3(b), is almost flat, but it displays a small ripple. This ripple can be attributed to the unstable phase shift of the TBPF imparted on the OC since the relative frequency between the OC and the TBPF is unstable.

Fig. 4 depicts the schematic configuration of the two-tap incoherent microwave photonic notch filter. Two distinct tunable laser sources (TLS1 and TLS2) were used in the experiment. They are naturally incoherent. Thus, the minimal time delay in the filter is not limited by the coherence length of the laser, and it makes possible to achieve a higher FSR for the filter. The frequency distance between two lasers was adjusted at 200 GHz (TLS1: 1549.935 nm, TLS2: 1551.535 nm) to avoid signal distortion caused by the beating signal between two lasers. The RF signal from the output port of the VNA was split by an RF power splitter. Then, the same two RF signals were applied to the DPMZM and a conventional signal-driver MZM. Light outputs from TLS1 and TLS2 were fed to the DPMZM and the signal-driver MZM, respectively. The real coefficient of the filter is generated in the lower arm with a path imbalance between the two taps. The upper arm was used to implement

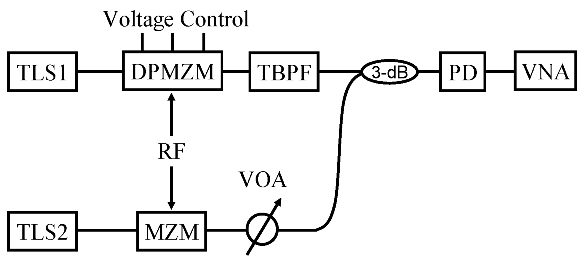

Fig. 4. Experimental setup of the two-tap microwave photonic notch filter with complex coefficient. TLS: tunable laser source. DPMZM: dual-parallel Mach–Zehnder modulator. TBPF: tunable optical bandpass filter. VOA: variable optical attenuator. PD: photodetector. VNA: vector network analyzer.

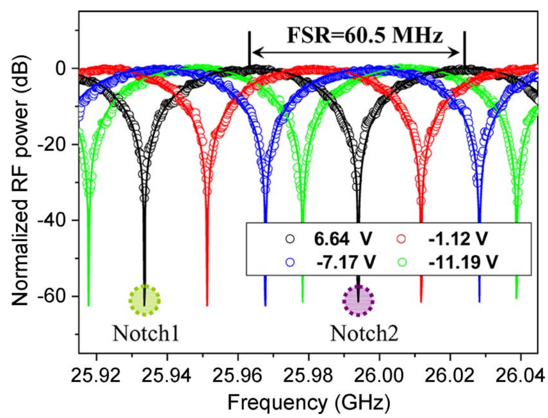

Fig. 5. Frequency response of the two-tap photonic filter with complex coefficient for different bias voltages (V_3) of the DPMZM. Circles, experimental results; solid curves, theoretical results obtained for fitted parameters.

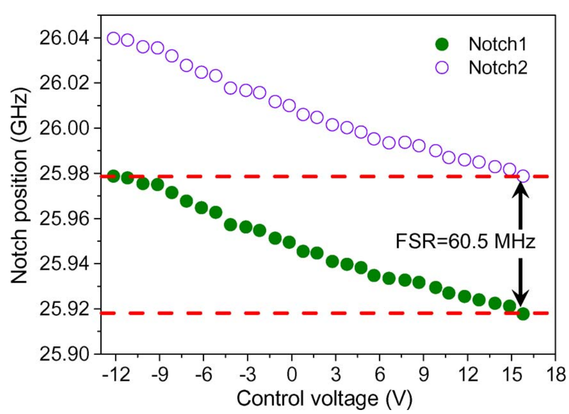

Fig. 6. Measured notch positions (marked as Notch1 and Notch2 in Fig. 4) of the photonic filter versus the bias voltages (V_3) of the DPMZM.

RF phase shifter that is needed to obtain a complex coefficient. A variable optical attenuator (VOA) was added in the lower arm to provide amplitude balance between the two arms. Then, the optical signals from two arms were combined to mutually interfere in the PD by a 3-dB optical coupler, and the filter frequency response was measured by the VNA.

Fig. 5 shows an excellent agreement of the measured and theoretical filter responses for different bias voltages (V_3) of the DPMZM. The FSR is 60.5 MHz, corresponding to 3.3-m optical fiber length difference between the two arms. Note that the notch position of the filter is tuned while maintaining the shape of the transfer function unaltered. Fig. 6 demonstrates that the notch positions (marked as Notch1 and Notch2 in Fig. 5) of the notch filter can be continuously tuned over the full FSR, without changing the spectral shape of the response, by adjusting the bias voltages (V_3) of the DPMZM.

4. Conclusion

We have demonstrated an incoherent microwave photonic notch filter with a complex coefficient. The complex coefficient is generated using a DPMZM and a TBPF. By simply controlling the bias voltage of the DPMZM, the frequency response of the filter can be continuously tuned over an entire FSR while maintaining the shape of the transfer function unchanged. The limitation of the RF phase shifter caused by the nonperfect transfer function of the TBPF has been analyzed. The calculated and the measured frequency responses of the notch filter exhibit excellent agreement.

References

[1] J. Capmany and D. Novak, "Microwave photonics combines two worlds," *Nat. Photon.*, vol. 1, no. 6, pp. 319–330, Jun. 2007.

[2] J. Sancho, S. Chin, M. Sagues, A. Loayssa, J. Lloret, I. Gasulla, S. Sales, L. Thévenaz, and J. Capmany, "Dynamic microwave photonic filter using separate carrier tuning based on stimulated Brillouin scattering in fibers," *IEEE Photon. Technol. Lett.*, vol. 22, no. 23, pp. 1753–1755, Dec. 2010.

[3] M. Sagues, A. Loayssa, and J. Capmany, "Multitap complex-coefficient incoherent microwave photonic filters based on stimulated Brillouin scattering," *IEEE Photon. Technol. Lett.*, vol. 19, no. 16, pp. 1194–1196, Aug. 2007.

[4] M. Sagues, R. G. Olcina, A. Loayssa, S. Sales, and J. Capmany, "Multi-tap complex-coefficient incoherent microwave photonic filters based on optical single-sideband modulation and narrow band optical filtering," *Opt. Express*, vol. 16, no. 1, pp. 295–303, Jan. 2008.

[5] T. Mengual, B. Vidal, and J. Martí, "Continuously tunable photonic microwave filter based on a spatial light modulator," *Opt. Commun.*, vol. 281, no. 10, pp. 2746–2749, May 2008.

[6] Y. Jin, X. Dong, J. Zhou, and P. P. Shum, "Continuously tunable microwave photonic notch filter based on the differential group delay," *Microw. Opt. Technol. Lett.*, vol. 53, no. 1, pp. 121–123, Jan. 2011.

[7] E. Hamidi, D. E. Leaird, and A. M. Weiner, "Tunable programmable microwave photonic filters based on an optical frequency comb," *IEEE Trans. Microw. Theory Tech.*, vol. 58, no. 11, pp. 3269–3278, Nov. 2010.

[8] G. Ning, S. Aditya, P. Shum, and J. Q. Zhou, "Switchable coherence-free microwave photonic notch filter using a pair of intensity modulators," *IEEE Photon. Technol. Lett.*, vol. 20, no. 4, pp. 261–263, Feb. 2008.

[9] K. Zhu, H. Ou, C. Ye, H. Fu, and S. He, "All-optical coherence-free microwave filter with switchable passbands based on phase and intensity hybrid modulation," *Opt. Commun.*, vol. 284, no. 1, pp. 140–143, Jan. 2011.

[10] Y. Yan and J. Yao, "Photonic microwave bandpass filter with improved dynamic range," *Opt. Lett.*, vol. 33, no. 15, pp. 1756–1758, Aug. 2008.

[11] Y. Yu, E. Xu, J. Dong, L. Zhou, X. Li, and X. Zhang, "Switchable microwave photonic filter between high Q bandpass filter and notch filter with flat passband based on phase modulation," *Opt. Express*, vol. 18, no. 24, pp. 25 271–25 282, Nov. 2010.

[12] F. Coppinger, S. Yegnanarayanan, P. D. Trinh, B. Jalali, and I. L. Newberg, "Nonrecursive tunable photonic filter using wavelength-selective true time delay," *IEEE Photon. Technol. Lett.*, vol. 8, no. 9, pp. 1214–1216, Sep. 1996.

[13] D. Pastor, J. Capmany, and B. Ortega, "Broadband tunable microwave transversal notch filter based on tunable uniform fiber Bragg gratings as slicing filters," *IEEE Photon. Technol. Lett.*, vol. 13, no. 7, pp. 726–728, Jul. 2001.

[14] N. You and R. A. Minasian, "A novel tunable microwave optical notch filter," *IEEE Trans. Microw. Theory Tech.*, vol. 49, no. 10, pp. 2002–2005, Oct. 2001.

[15] Y. Yan and J. Yao, "A tunable photonic microwave filter with a complex coefficient using an optical RF phase shifter," *IEEE Photon. Technol. Lett.*, vol. 19, no. 19, pp. 1472–1474, Oct. 2007.

[16] A. Loayssa, J. Capmany, M. Sagues, and J. Mora, "Demonstration of incoherent microwave photonic filters with all-optical complex coefficients," *IEEE Photon. Technol. Lett.*, vol. 18, no. 16, pp. 1744–1746, Aug. 2006.

[17] W. Xue, S. Sales, J. Mork, and J. Capmany, "Widely tunable microwave photonic notch filter based on slow and fast light effects," *IEEE Photon. Technol. Lett.*, vol. 21, no. 3, pp. 167–169, Feb. 2009.

[18] M. Pu, L. Liu, W. Xue, Y. Ding, L. H. Frandsen, H. Ou, K. Yvind, and J. M. Hvam, "Tunable microwave phase shifter based on silicon-on-insulator microring resonator," *IEEE Photon. Technol. Lett.*, vol. 22, no. 12, pp. 869–871, Jun. 2010.

[19] X. Li, J. Dong, Y. Yu, and X. Zhang, "A tunable microwave photonic filter based on an all-optical differentiator," *IEEE Photon. Technol. Lett.*, vol. 23, no. 5, pp. 308–310, Mar. 2011.

[20] S. Li, X. Zheng, H. Zhang, and B. Zhou, "Compensation of dispersion-induced power fading for highly linear radio-over-fiber link using carrier phase-shifted double sideband modulation," *Opt. Lett.*, vol. 36, no. 4, pp. 546–548, Feb. 2011.